Photocatalytic Reduction of Ni (II) Ions Using Low Amounts of Titania Nanoparticles: RSM Modelling, Kinetic

Javad Saien [1], Amir Azizi[1], Ali Reza Soleymani [2]*

Received: 09.02.2014 *Accepted: 30.03.2014*

ABSTRACT

Background: Heavy metals in aquatic systems usually interfere with many beneficial uses of water. Divalent nickel is a commonly occurring toxic metal in natural ecosystems due to the effluent of refineries, electroplating, and casting industries. In aquatic environments, nickel appears as Ni (II) and Ni^0. Despite the high reported toxicity for Ni (II), Ni^0 is only slightly toxic. Various methods have been proposed for the treatment of aqueous solutions containing Ni (II). Photocatalytic reduction is an important process; titanium dioxide has been mostly used as a very efficient photocatalyst.

Methods: In this study, the removal of divalent nickel ions in aqueous solutions was studied in the presence of remarkably low dosages of nano-titania photocatalyst. Direct imposed irradiation was utilized for treatment of solutions. Accordingly, the influence of four operational parameters, including temperature within the conventional range of 20 to 40 °C, was investigated. Design of experiments, modeling and process optimization were accomplished using central composite design of response surface methodology.

Results: Reduced quadratic expression was developed for the reduction efficiency (*RE*), and the analysis of variance showed its capability in reproducing the data. The effectiveness of each parameter was determined. At the best found conditions of [TiO_2] = 42 mg/L, pH = 9.2, *T* = 34 °C and after 90 minutes of treatment, about 85% removal was achieved for initial 5 mg/L nickel solutions. Pseudo first order reactions proceeded.

Conclusion: Based on CCD method, the influence of individual operating parameters and their interactions were obtained. A quadratic equation predicted the variations quite well.

Keywords: Divalent Nickel, Kinetic, Modelling, Nano-Titania, Photocatalytic Process.

IJT 2014; 1136-1144

INTRODUCTION

Heavy metals in aquatic systems usually interfere with many beneficial uses of water. Metal ions have infinite lifetime and can be accumulated in food chains to a toxic level [1]. Divalent nickel is a commonly occurring toxic metal in natural ecosystems due to the effluent of refineries, electroplating, casting industries, storage batteries, and nickel-plating plants [2, 3]. High nickel concentrations cause lung cancer, and nose and bone dermatitis (nickel itch) while its acute concentrations cause dizziness, headache, nausea, vomiting, chest pain, cough and breathing problems, cyanosis, extreme weakness, and DNA damage [4, 5]. In aquatic environments, nickel appears as Ni(II) and Ni^0 [6, 7]. However, the high reported toxicity for Ni(II), Ni^0 is only slightly toxic [8].

Various methods have been proposed for the treatment of aqueous solutions containing Ni(II), e.g. precipitation, ion exchange, electrolysis, adsorption and photocatalysis [9-11]. In the last key process, titanium dioxide has been mostly used, as very efficient photocatalyst because of non-toxicity, low cost, and chemically stability [12]. As documented in the literature, the main step in this process is the formation of electron-hole pairs ($e^-_{CB} - h^+_{VB}$) on the catalyst surface upon irradiation with the proper photon energy to overcome the band gaps. The electron-hole pairs are then separated between the valance and conduction bands, and the adsorbed species (reactants) on the sites of catalyst undergo photo-induced oxidation reduction or even synthesis.

1. Department of Applied Chemistry, Bu-Ali Sina University, Hamedan, Iran.
2. Department of Applied Chemistry, Malayer University, Malayer, Iran.
*Corresponding Author:E-mail: zeaodin@yahoo.com

The semiconductor TiO_2 contains sufficient reducing power to induce nickel ion reduction. It is because the band gap of TiO_2 is around 3.2 eV with the energy of conduction band -0.3 eV and valence band +2.9 eV at pH 5.6 [13]. Hence, any metal ion having a reduction potential less negative than −0.3 eV would be potentially reduced by photo-generated electrons of TiO_2. The reduction of metal ions, such as Cu(II), Cr(VI), Au(III), and Ag(I) (reduction potentials usually less than -0.5 eV) have been widely studied in the presence of TiO_2 [13–16]. The reduction of metal ions normally occurs by capturing the photo–excited conduction band electrons while water or other organics are oxidized by the valence band holes. The following reactions can describe the Ni(II) reduction process [8]:

$$2[TiO_2 \xrightarrow{h\nu} e^- + h^+] \quad (1)$$

$$Ni^{2+} + 2e^- \rightarrow Ni^0 \quad (2)$$

$$H_2O + 2h^+ \rightarrow \frac{1}{2}O_2 + 2H^+ \quad (3)$$

$$Ni^{2+} + H_2O + h^+ \rightarrow Ni^0 + \frac{1}{2}O_2 + 2H^+ \quad (4)$$

To date, some investigations on photo-reduction of Ni(II) have been reported, all with very high levels of nano TiO_2 concentration within 250-2000 mg/L [8,17-19]. In the present study, proceeding with very low amounts of titania was targeted. Low dosage catalyst consumption is much practically interesting due to separation and regeneration problems. The influence of temperature, on the other hand, is taken into account in this study; a case that has not been reported so far. Indeed, direct heating is beneficial in process intensification with no extra reagent addition or using special devices. Temperature within conventional range can play an important role in altering the performance of these processes, as long as economic evaluation shows favorite results. This parameter as well as solution pH, TiO_2 dosage, and reaction time are considered and the corresponding modeling is obtained via response surface methodology (RSM). The best operating conditions are estimated and then validated with confirmatory experiments. Accordingly, the perfect reaction kinetic is determined for the overall conducted reaction.

MATERIALS AND METHODS

All reagents and chemicals used in this study were analytical grade and they were used as received from the suppliers. Nickel nitrate hexa aqua, as the source of Ni(II) was Merck product. Used in analytical procedure, 1-(2-Pyridylazo)-2-naphthol (PAN), ethanol and Triton X-100 were all Merck products. Sulfuric acid and sodium hydroxide for pH adjustment were also purchased from Merck. Titanium dioxide nano particles (P-25 purity>99.5%) were supplied by Plasma Chem with BET surface area of 50 m^2/g and the average particle diameter of 21nm. All aqueous solutions were prepared using deionized water with conductivity less than 0.08 µS/cm.

A cylindrical photo-reactor made of glossy stainless steel with 1.25 L capacity was used. The light source was a 250 W mercury lamp with the wavelength range of 280–400 nm and the maximum emission of 365 nm, located centrally in the reaction media with perfect light utilization. In order to mix the reactor content well and achieve fine dispersion of the catalyst particles, an ultrasound source (28 kHz, 60 W) was placed at the outside bottom of the reactor. The desired reaction temperature was adjusted and maintained constant via a stainless steel water-flow jacket, connected to a thermostat bath.

To run each experiment, a solution (1 L) of 5.0 mg/L of Ni(II) ions was prepared and after adjustment of pH (using sulfuric acid and sodium hydroxide dilute solutions), it was transferred into the reactor and then temperature was set to the desired level. The needed amount of the catalyst particles was added and, prior to light irradiation, the suspension was sonicated for 5 min and then maintained under mixing for 30 min in dark to ensure adsorption/desorption equilibria. The maximum substrate adsorption was as low as 4%, which was subtracted from the initial concentration.

To follow the reaction progress, 2.5 mL samples were withdrawn at different times. Separation of the titania nano-particles was then performed with vigorous centrifugation. The residual concentration of Ni(II) ions was analyzed via colorimetery using PAN as the color agent [20]. Accordingly, the best complex formation conditions were prepared with 2.5 mL

of 1.0% triton X-100 water solution, 2 mL of universal buffer solution (pH 8.5), 1.0 mL of 0.01% PAN solution in ethanol, together with 2 mL of collected sample, all added into a 10 mL standard flask, while volume was made up to the mark with deionized water. A maximum wavelength absorbance with UV-visible spectrometer is corresponding for the produced nickel complex at maximum wavelength of 568 nm. Based on appropriate calibration data, the reduction efficiency (*RE*) of Ni(II), at any time was obtained as:

$$RE = \frac{[\mathrm{Ni(II)}]_{\circ} - [\mathrm{Ni(II)}]_{t}}{[\mathrm{Ni(II)}]_{\circ}} \times 100 \quad (5)$$

Where $[Ni(II)]_o$ and $[Ni(II)]_t$ are initial and appropriate time concentrations (in mg/L), respectively.

RESULTS

Design of Experiments and Model

The essential parameters of catalyst loading, pH, temperature, and reaction time, were considered and the central composite design (CCD) methodology was applied. In this regard, a four-factor, five-level CCD was employed. Each of the variables were assessed at five different levels of factorial points (-1, +1), axial points ($-\alpha, +\alpha$), and central point (0). Table 1 presents the range of these variables which were chosen based on some preliminary experiments. The experimental design matrix is depicted in Table 2.

Design-Expert software (version 8.0.5) was used to determine the best mathematical expression of the process efficiency. Based on statistical items, a quadratic model was suggested in the form:

$$y = \beta_0 + \sum_{i}^{m} \beta_i x_i + \sum_{i}^{m} \beta_{ii} x_i^2 + \sum_{i}^{m-1} \sum_{j=i+1}^{m} \beta_{ij} x_i x_j + \varepsilon \quad (6)$$

Where *y* stands for predicted response (*RE*), β_0 the constant coefficient, β_i the linear coefficients, β_{ii} the quadratic coefficients, β_{ij} the interaction coefficients and x_i, x_j are the influencing process variables, *m* is the number of variables, and ε is the residual error.

The significance of the model terms can be evaluated based on the "P>*F*" at the 95% confidence level. Contributed terms with "*P>F*" less than 0.05 are statistically significant. Consequently, the insignificant quadratic and interaction terms ($x_{TiO_2}x_t$, $x_{TiO_2}x_T$, $x_T x_t$ and x_t^2) were omitted to modify the model in the following form:

$$RE = 30.69 + 22.80xpH + 10.0xTio2 + 3.52xT + 7.13xt + 6.33xpHxTio2 + 2.22xpHxT + 2.46xtxpH + 3.53x2pH + 2.15x2Tio2 - 2.42x2T \quad (7)$$

The analysis of variance (ANOVA) was then carried (see Table 3). The above reduced equation gives a coefficient of determination (R^2) value of 0.987, and the Adj-R^2 (modified R^2, adjusted for the number of explanatory terms in the model) value of 0.981 which is very close to the corresponding R^2 value that indicates a reasonable proportion between the number of model terms and the modified model. Also, pred-R^2 (how well the model predicts responses for new observations) of 0.966 is in reasonable agreement with the Adj-R^2. Furthermore, "*P>F*" (model mean square divided by residual mean square) [21] less than 0.0001 and the high *F*-value of 151.6 imply that Eq. (7) is satisfactory. Moreover, the feature of the model can be seen in Figure 1, indicating an agreement between the model prediction and experimental data.

Table 1. The ranges and levels of the used variables in terms of the real and coded factors.

Variables	Levels and ranges				
	$-\alpha$	(−1)	(0)	(+1)	$+\alpha$
pH, x_{pH}	7.2	7.5	8.35	9.2	9.55
[TiO_2] (mg/L), x_{TiO_2}	1.0	8.0	25.0	42.0	49.1
Temperature (°C), x_T	16.7	20.0	28.0	36.0	39.3
Reaction time (min), x_t	53.8	60.0	75.0	90.0	96.2

Table 2. The 4-factor CCD matrix consisting of the empirical and model predicted values of the response.

Runs	Design factor				*RE*	
	pH	[TiO_2] (mg/L)	*T* (°C)	*t* (min)	Exp	Pred.
1	8.35	25	28	53.8	21.1	20.8
2	8.35	25	28	75	28.8	30.9
3	8.35	25	28	75	32.5	30.9
4	9.2	8	20	60	25.4	26.6
5	8.35	25	28	75	32.1	30.9
6	8.35	25	16.7	75	17.3	20.9
7	7.5	42	20	60	12.8	10.4
8	7.5	8	36	90	14.6	15.1
9	8.35	25	28	75	28.7	30.9
10	9.2	8	20	90	43.5	42.7
11	7.5	42	36	90	20.1	22.3
12	8.35	1	28	75	20.2	20.9
13	8.35	25	28	75	30.1	30.9
14	8.35	25	39.3	75	33.3	30.8
15	7.2	25	28	75	4.4	5.6
16	9.55	25	28	75	70.1	70.1
17	7.5	42	20	90	17.9	16.6
18	7.5	8	36	60	4.5	2.5
19	9.2	42	20	90	73.8	75.3
20	9.2	42	36	90	86.3	89.9
21	8.35	49.1	28	75	48.6	49.2
22	9.2	8	36	60	32.9	34.9
23	8.35	25	28	96.2	46.2	41.1
24	9.2	42	20	60	63.6	59.3
25	8.35	25	28	75	29.3	30.9
26	9.2	8	36	90	60.1	57.3
27	9.2	42	36	60	68.5	67.6
28	7.5	8	20	90	9.7	9.3
29	7.5	42	36	60	9.3	9.9
30	7.5	8	20	60	2.1	3.1

Table 3. ANOVA for the reduced quadratic model[a].

Source	Sum of squares	Degree of freedom	Mean square	*F*-Value	Prob>*F*
model	14686.48	10	1468.65	151.6	< 0.0001
X_{pH}	10394.21	1	10394.21	1072.96	< 0.0001
X_{Tio2}	1999.21	1	1999.21	206.37	< 0.0001
X_T	247.95	1	247.95	25.6	< 0.0001
X_t	1017.87	1	1017.87	105.07	< 0.0001
$X_{pH}X_{Tio2}$	640.09	1	640.09	66.07	< 0.0001
$X_{pH}X_T$	78.59	1	78.59	8.11	0.0103
$X_{pH}X_t$	96.43	1	96.43	9.95	0.0052
X^2_{PH}	119.60	1	119.60	12.35	0.0023
X^2_{Tio2}	44.57	1	44.57	4.6	0.0451
X^2_T	56.36	1	56.36	5.82	0.0261
Residual	184.06	19	9.69		
Lack of Fit	160.71	14	11.48	2.46	0.1638
Pure Error	23.35	5	4.67		
Cor Total	14870.54	29			

[a] R^2= 0.987, adj-R^2 = 0.981, pred-R^2= 0.966

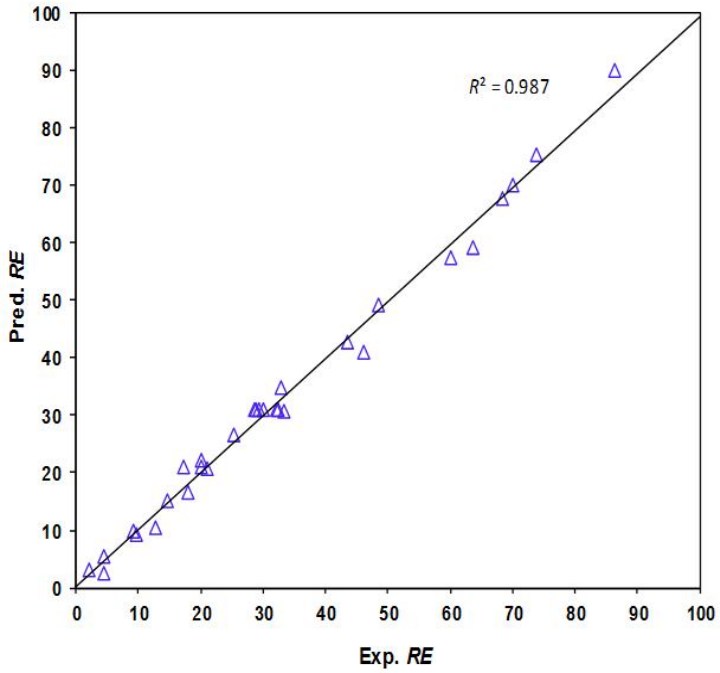

Figure 1. The model predicted RE values versus experimental values.

DISCUSSION

The Impact of Parameters

The influence of operating parameters are presented via three dimensional response surface plots (Figure 2 a, b and c). In each plot, two variables were kept constant (at the related zero levels) and the variation of *RE* was depicted versus the other two. This way, the interactions between variables were evaluated.

Figure 2 (a) shows the influence of pH and TiO_2 dosage on the photo-reduction process. *RE* increases with pH, in particular alkaline conditions, but the effect is significant at high TiO_2 dosages. This reveals the presence of an interaction between them at "*P*>*F*" value less than 0.0001, according to the "$x_{pH}x_{TiO_2}$" term in Table 3.

The pH of zero point charge (pH_{ZPC}) of TiO_2 (p-25 product) is 6.8 [22, 23]. The catalyst surface is, therefore, positively charged at pHs<pH_{ZPC} and negatively charged at pHs>pH_{ZPC}. As pH increases, TiO_2 surface is more negatively charged, leading to higher adsorption of Ni (II) ions and, thus, higher *RE* achievement [24]. Hence, at neutral pH, there is a low tendency for adsorption of Ni(II) ions, and the process does not exhibit any catalyst dosage dependence.

Figure 2 (b) shows that the influence of temperature on the process is different. Under neutral pH, where adsorption of Ni(II) ions on the catalyst surface is the limiting step, the effect of temperature is nil. However, under alkaline pH, *RE* increases with increase of temperature up to 34 °C and then remains almost constant.

Figure 2(c) depicts the effect of the reaction time and pH on *RE*. Higher reaction times provide higher reduction efficiency but the trend of variation is different around neutral and alkaline pHs. This behaviour corresponds to the vital role of Ni (II) adsorption onto the catalyst surface.

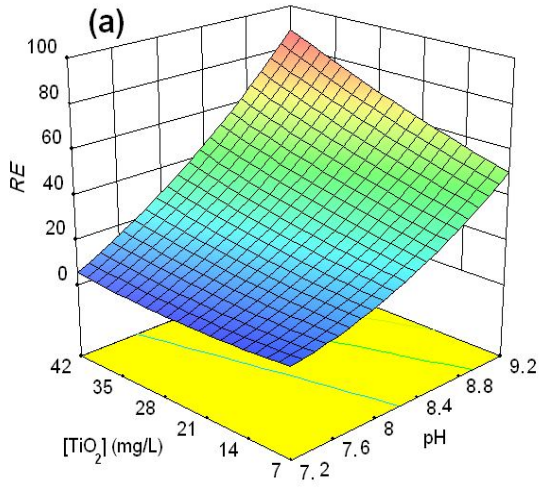

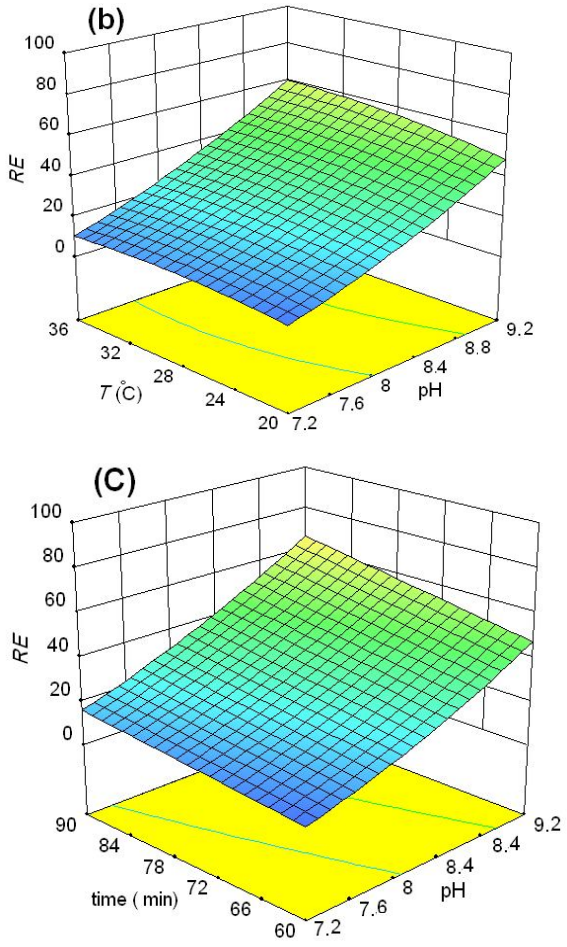

Figure 2. The response surface plots showing the effect of: (a) TiO2 particles dosage and solution pH at temperature of 28 °C and reaction time of 75 min (central point), (b) temperature and pH with TiO2 particles dosage of 25 mg/L and reaction time of 75 min, (c) reaction time and pH at temperature of 28 °C and TiO2 dosage of 25 mg/L.

Optimization

By screening these variations, a maximum 86.4% Ni(II) reduction is predictable from the model with titania loading of about 42 mg/L, and other conditions (pH 9.2, temperature of 34 °C, and the 90-min reaction process). The confirmatory experimental run under these conditions showed a reduction efficiency of 84.5%. This close agreement confirms the model weight.

To investigate the contributing reaction branches in the process; experiments were conducted under optimum conditions either in the presence of TiO_2 nanoparticles (photocatalysis) or in their absence (photolysis). The trend of Ni(II) concentration variations during the processes time can be seen in Figures 3 (a) and 3(b) compares *RE* values after two typical times, for both cases. The *RE* exceeds 54 % and 84% in the case of photocatalysis and 19% and 41% in the case of photolysis after 30 and 90 min, respectively. This shows that photocatalysis operates significantly more effectively than only photolysis; however, UV light alone is efficient in this regard.

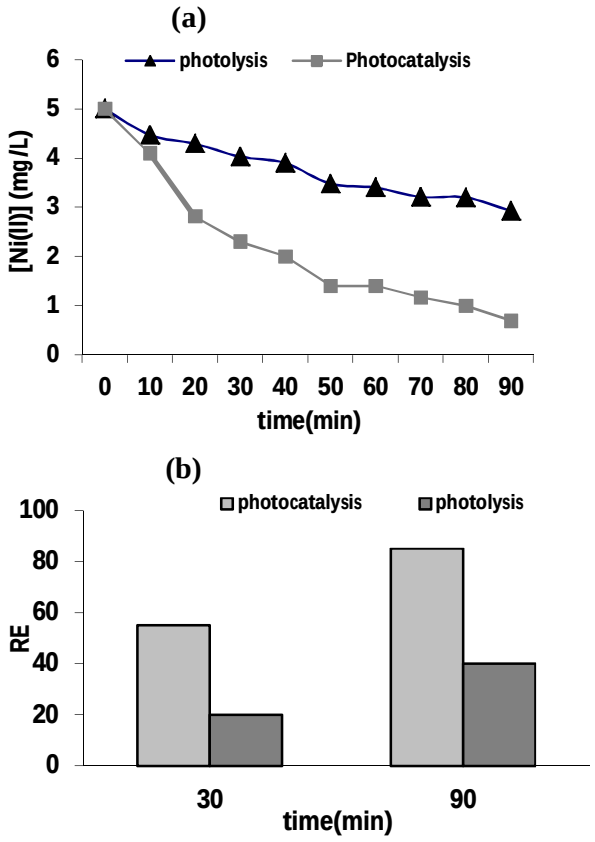

Figure 3. The variation of Ni(II) concentration versus time (a), and comparison of *RE* values after two different times (b) for the photolysis and photocatalysis processes; pH = 9.2, [TiO_2] = 42 mg/L, and T = 34 °C.

Photocatalyst Structure Analysis

The presence of zero valent nickel as well as its oxide (NiO) was detected by high-resolution XPS analysis of TiO_2 particles, collected after the reaction. The Ni 2p peaks and the satellites show the presence of these two species of nickel. The spectrum of Ni^0 fits by broad peaks at 853.6 and 870.9 eV [25], and the NiO by Ni 2p peaks at 857.6 and 874.2 eV [26] (indicated by arrows in Figure 4).

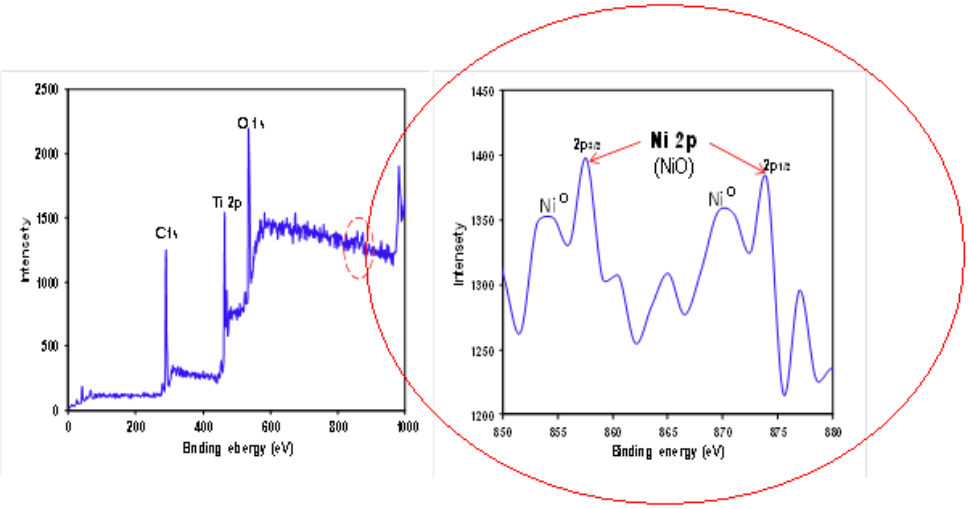

Figure 4. XPS spectrum of Ni 2p peaks and satellites for TiO_2 particles after reduction process.

Kinetic Study

Owing to practical applications, the photocatalytic reduction kinetic of Ni(II) ions was investigated under the optimum conditions of pH 9.2, TiO_2 concentration of 42 mg/L, and different applicable temperatures of 20, 25, 30, 35 and 40 ^{0}C. In this regard, the concentration of Ni(II) ions was measured at different times.

Here, a preliminary power law kinetic model was used for modeling the experimental data [27, 28]:

$$r = -\frac{\mathrm{d}[\mathrm{Ni(II)}]}{\mathrm{d}t} = k[\mathrm{Ni(II)}]^n \qquad (8)$$

where r, t, k, and n are the rate of reduction, reaction time, rate constant and the order of reaction, respectively. As it is known, according to the Arrhenius equation, the rate constant of most reactions is related to temperature by $k = k_0 e^{-E_a/RT}$, where k_o, E_a and $R$are frequency factor, activation energy and the universal constant of gasses, respectively. Equation (8) can, therefore, be written as:

$$\ln r = \ln k_0 - \frac{E_a}{R}\frac{1}{T} + n\ln[\mathrm{Ni(II)}] \qquad (9)$$

The differential method of analysis, based on the provided data of concentration at different times was employed for finding the rate at each appropriate concentration. The goodness of fitting in agreement with Equation (9) is shown in Figure 5. In this figure, experimental data are marked with bold dots and the fitted equation with a meshed plane. Activation energy and kinetic parameters of the used reduction process along with the coefficient of determination (R^2) are given in Table 4.

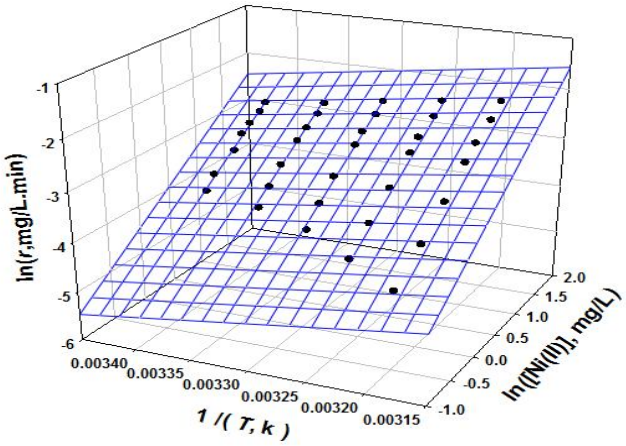

Figure 5. Correlation diagram for experimental kinetic data, pH of 9.2, and [TiO_2] = 42 mg/L.

Table 4. Kinetic parameters of the Ni(II) photocatalytic reduction, pH of 9.2, and [TiO_2] = 42 mg/L.

k_0	E_a	n	R^2
3.06×10^2 (mg/L)/min	24.54 (kJ/mol)	1.0	0.991

CONCLUSION

This study illustrated the feasibility of photocatalytic reduction of Ni(II) with very low

amounts of titania nanoparticles when the influence of temperature is also involved. Based on CCD methodology, the influence of individual operating parameters and their interactions were obtained. A quadratic equation predicted the variations quite well. Accordingly, the best operating conditions were: pH = 9.2, $[TiO_2]$ = 42 mg/L and T = 34 °C. Applying the pertinent conditions, about 85% reduction efficiency was achieved after 90 min treatment. Moreover, confirmatory analysis of photocatalyst particles indicated the separation of nickel zero valence species from the nickel solutions. Kinetic studies revealed pseudo first order reactions for overall conducted reaction.

ACKNOWLEDEGMENTS

The authors wish to acknowledge the university authorities for the financial support of this study.

REFERENCES

1. Yun-nen C, Li-yuan C, editors. Comparison for adsorption modeling of heavy metals (Cd, Pb, Cu, Zn) from aqueous solution by bio-formulation. Bioinformatics and Biomedical Engineering. 2008; 16: 3248-51.
2. Xu H, Liu Y, Tay J-H. Effect of pH on nickel biosorption by aerobic granular sludge. Bioresource technology. 2006;97(3):359-63.
3. Samarghandi M, Azizian S, Siboni MS, Jafari S, Rahimi S. Removal of divalent nickel from aqueous solutions by adsorption onto modified holly sawdust: equilibrium and kinetics. Iranian Journal of Environmental Health Science & Engineering. 2011;8(2):167-74.
4. Veli S, Alyüz B. Adsorption of copper and zinc from aqueous solutions by using natural clay. Journal of Hazardous Materials. 2007;149(1):226-33.
5. Caicedo M, Jacobs JJ, Reddy A, Hallab NJ. Analysis of metal ion-induced DNA damage, apoptosis, and necrosis in human (Jurkat) T-cells demonstrates Ni2+ and V3+ are more toxic than other metals: Al3+, Be2+, Co2+, Cr3+, Cu2+, Fe3+, Mo5+, Nb5+, Zr2+. Journal of Biomedical Materials Research Part A. 2008;86(4):905-13.
6. Barakat M, Chen Y, Huang C. Removal of toxic cyanide and Cu (II) Ions from water by illuminated TiO2 catalyst. Applied Catalysis B: Environmental. 2004;53(1):13-20.
7. Chen D, K Ray A. Removal of toxic metal ions from wastewater by semiconductor photocatalysis. Chemical Engineering Science. 2001;56(4):1561-70.
8. Shirzad Siboni M, Samadi M-T, Yang J-K, Lee S-M. Photocatalytic removal of Cr (VI) and Ni (II) by UV/TiO2: kinetic study. Desalination and Water Treatment. 2012;40(1-3):77-83.
9. Malkoc E, Nuhoglu Y. Removal of Ni (II) ions from aqueous solutions using waste of tea factory: Adsorption on a fixed-bed column. Journal of Hazardous Materials. 2006;135(1):328-36.
10. Lacour S, Bollinger J-C, Serpaud B, Chantron P, Arcos R. Removal of heavy metals in industrial wastewaters by ion-exchanger grafted textiles. Analytica chimica acta. 2001;428(1):121-32.
11. Wu W, Peng J-J. Linear control of electrochemical tubular reactor system—Removal of Cr (VI) from wastewaters. Journal of the Taiwan Institute of Chemical Engineers. 2011;42(3):498-505.
12. Bhatkhande DS, Pangarkar VG, Beenackers AA. Photocatalytic degradation for environmental applications–a review. Journal of Chemical Technology and Biotechnology. 2002;77(1):102-16.
13. Blake DM, Webb J, Turchi C, Magrini K. Kinetic and mechanistic overview of TiO2-photocatalyzed oxidation reactions in aqueous solution. Solar Energy Materials. 1991;24(1):584-93.
14. Prairie MR, Evans LR, Stange BM, Martinez SL. An investigation of titanium dioxide photocatalysis for the treatment of water contaminated with metals and organic chemicals. Environmental Science & Technology. 1993;27(9):1776-82.
15. Foster NS, Noble RD, Koval CA. Reversible photoreductive deposition and oxidative dissolution of copper ions in titanium dioxide aqueous suspensions. Environmental Science & Technology. 1993;27(2):350-6.
16. Herrmann J-M, Disdier J, Pichat P. Photocatalytic deposition of silver on powder titania: consequences for the recovery of silver. Journal of Catalysis. 1988;113(1):72-81.
17. Joshi KM, Patil BN, Shirsath DS, Shrivastava VS. Photocatalytic removal of Ni (II) and Cu (II) by using different Semiconducting materials. Advances in Applied Science Research. 2011;2(3):445-54.
18. Kabra K, Chaudhary R, Sawhney R. Solar photocatalytic removal of Cu (II), Ni (II), Zn (II) and Pb (II): Speciation modeling of metal–citric acid complexes. Journal of Hazardous Materials. 2008;155(3):424-32.
19. Kabra K, Chaudhary R, Sawhney R. Effect of pH on solar photocatalytic reduction and deposition of Cu (II), Ni (II), Pb (II) and Zn (II): Speciation

modeling and reaction kinetics. Journal of Hazardous Materials. 2007;149(3):680-5.
20. Awwa A. Standard methods for the examination of water and wastewater. Washington, DC Standard Methods for the Examination of Water and Wastewater. 1998;20.
21. Sakkas VA, Islam MA, Stalikas C, Albanis TA. Photocatalytic degradation using design of experiments: a review and example of the Congo red degradation. Journal of Hazardous Materials. 2010;175(1):33-44.
22. Ollis DF, Pelizzetti E, Serpone N. Photocatalyzed destruction of water contaminants. Environmental Science & Technology. 1991;25(9):1522-9.
23. Pujara K, Kamble SP, Pangarkar VG. Photocatalytic degradation of phenol-4-sulfonic acid using an artificial UV/TiO2 system in a slurry bubble column reactor. Industrial & engineering chemistry research. 2007;46(12):4257-64.
24. Kabra K, Chaudhary R, Sawhney R. Solar photocatalytic removal of metal ions from industrial wastewater. Environmental Progress. 2008;27(4):487-95.
25. Grosvenor AP, Biesinger MC, Smart RSC, McIntyre NS. New interpretations of XPS spectra of nickel metal and oxides. Surface Science. 2006;600(9):1771-9.
26. Prieto P, Nistor V, Nouneh K, Oyama M, Abd-Lefdil M, Díaz R. XPS study of silver, nickel and bimetallic silver–nickel nanoparticles prepared by seed-mediated growth. Applied Surface Science. 2012;258(22):8807-13.
27. Saien J, Soleymani A. Degradation and mineralization of Direct Blue 71 in a circulating upflow reactor by UV/TiO2process and employing a new method in kinetic study. Journal of Hazardous Materials. 2007;144(1):506-12.
28. Saien J, Ojaghloo Z, Soleymani A, Rasoulifard M. Homogeneous and heterogeneous AOPs for rapid degradation of Triton X-100 in aqueous media via UV light, nano titania hydrogen peroxide and potassium persulfate. Chemical Engineering Journal. 2011;167(1):172-82.